

On-chip clearing for live imaging of 3D cell cultures: supplement

TINGTING YU,^{1,2,†} XIANG ZHONG,^{1,2,†} QIHANG YANG,^{1,2} CHAO GAO,^{1,2} WENYUE CHEN,^{1,2} XIANG LIU,^{1,2} ZHANG LIU,^{1,2} TINGTING ZHU,^{2,3} DONGYU LI,^{2,3} PENG FEI,^{2,3} ZAOZAO CHEN,^{4,5} ZHONGZE GU,^{4,5} AND DAN ZHU^{1,2,*}

¹Britton Chance Center for Biomedical Photonics - MoE Key Laboratory for Biomedical Photonics, Huazhong University of Science and Technology, Wuhan, Hubei 430074, China

²Wuhan National Laboratory for Optoelectronics - Advanced Biomedical Imaging Facility, Huazhong University of Science and Technology, Wuhan, Hubei 430074, China

³School of Optical and Electronic Information, Huazhong University of Science and Technology, Wuhan, Hubei 430074, China

⁴State Key Laboratory of Bioelectronics, School of Biological Science and Medical Engineering, Southeast University, Nanjing, Jiangsu 210096, China

⁵Institute of Biomaterials and Medical Devices, Southeast University, Suzhou, Jiangsu, 215163, China

[†]These authors contributed equally to this work.

*dawnzh@mail.hust.edu.cn

This supplement published with Optica Publishing Group on 31 May 2023 by The Authors under the terms of the [Creative Commons Attribution 4.0 License](https://creativecommons.org/licenses/by/4.0/) in the format provided by the authors and unedited. Further distribution of this work must maintain attribution to the author(s) and the published article's title, journal citation, and DOI.

Supplement DOI: <https://doi.org/10.6084/m9.figshare.22778384>

Parent Article DOI: <https://doi.org/10.1364/BOE.489219>

Supplementary Information

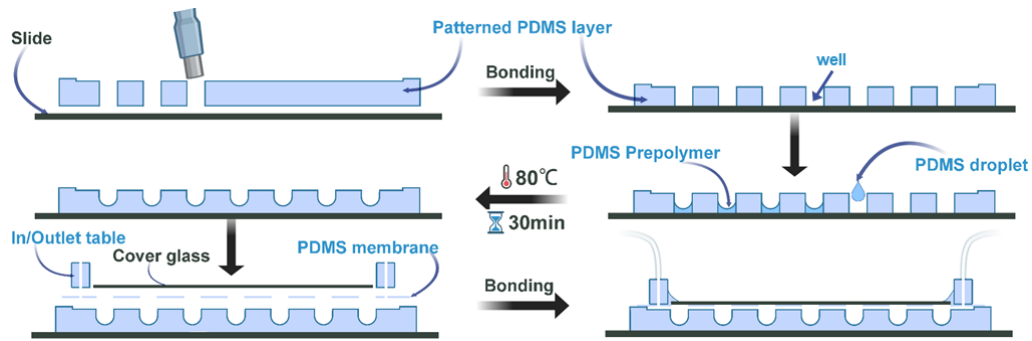


Fig. S1. Fabrication workflow of the culture and clearing arrays.

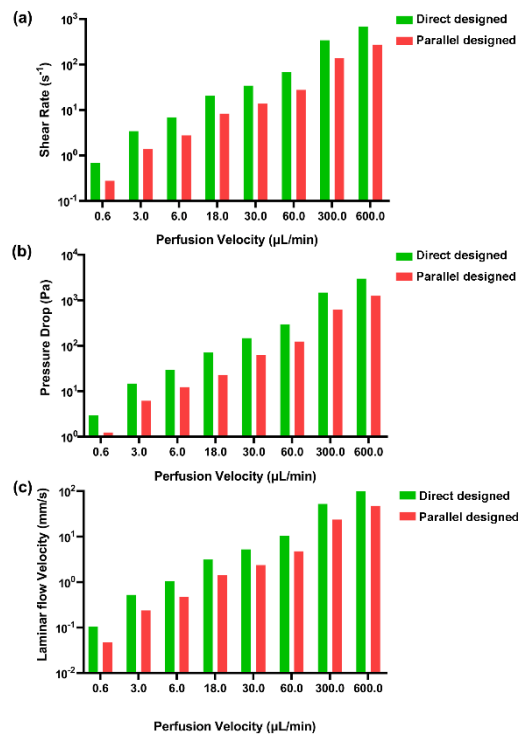


Fig. S2. Simulation results of the fluid parameters in different designed chips. (a) The shear rate. (b) The pressure drop. (c) The laminar flow velocity.

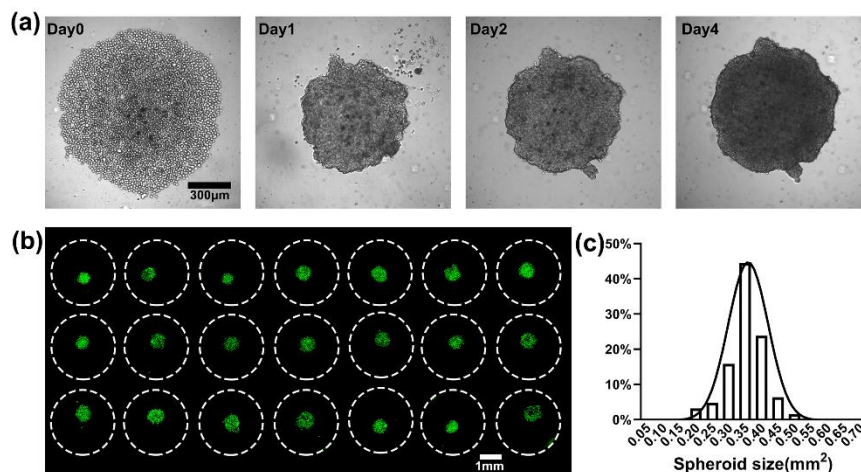


Fig. S3. Formation of 3D cell culture on the chip. (a) Bright-field images of MCF-7 tumor spheroids at 0d, 1d, 2d, and 4d during the culture on the chip. (b) The fluorescence images of cultured spheroids at 4d on the chip. (c) Size distribution of the 3D spheroids.

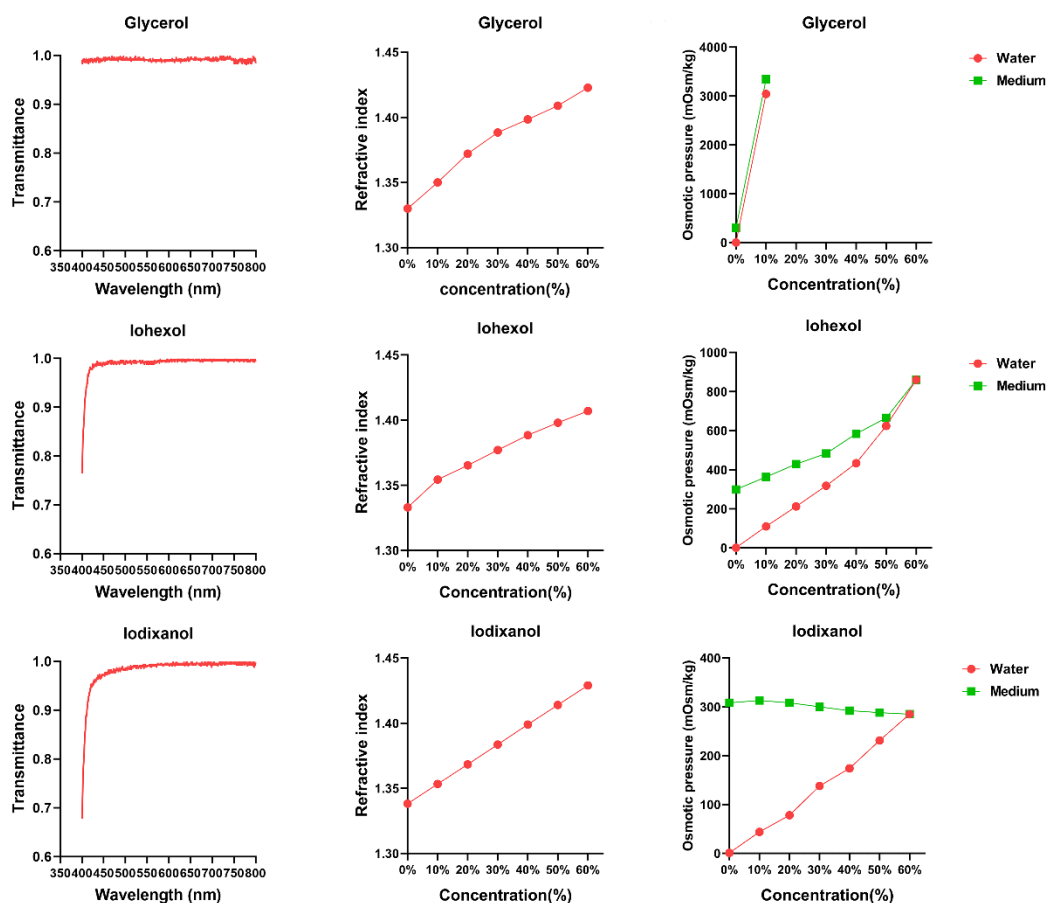


Fig. S4. Physicochemical properties of glycerol, iohexol and iodixanol solutions.

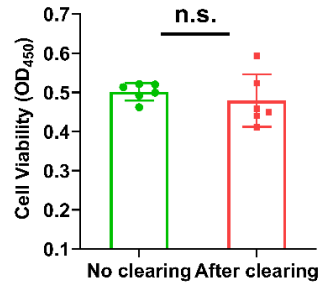


Fig. S5. Cell viability after 2 hours clearing.

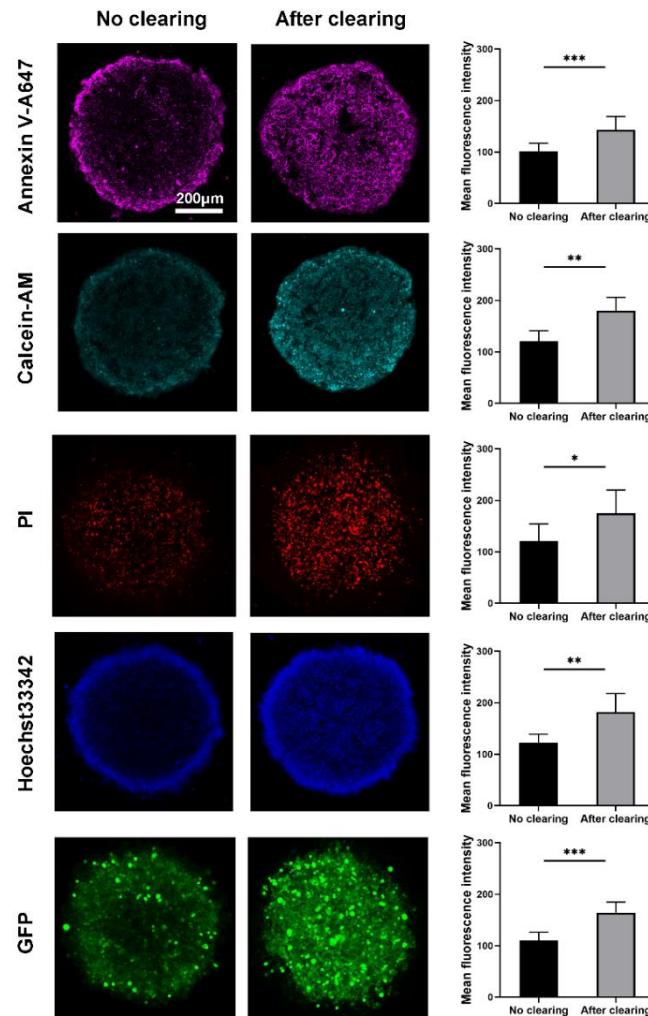


Fig. S6. Assessment of fluorescence compatibility of several commonly used fluorescent probes with the clearing agent, including Annexin-V-Alexa Fluor 647, Calcein-AM, PI, Hoechst 33342, and GFP.

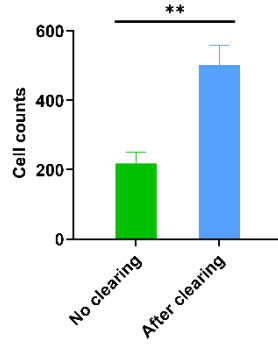


Fig. S7. Cell counts at the depth of 60 μm before and after clearing, $n=3$ (n indicates spheroid number).

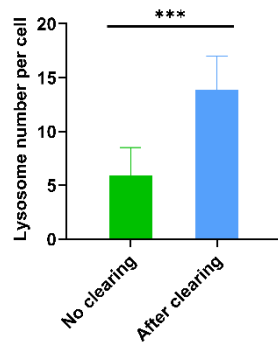


Fig. S8. Lysosome number in each cell detected before and after clearing, $n=9$ for no clearing and $n=15$ for after clearing (n indicates cell number).

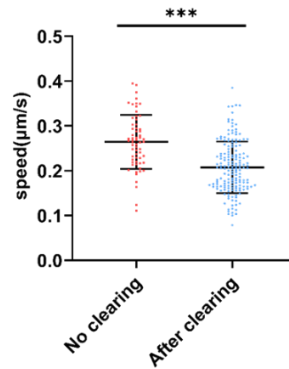


Fig. S9. Lysosome motility observed before and after clearing at the depth of 60 μm , $n=63$ for no clearing and $n=171$ for after clearing (n indicates lysosome number).

Movie S1. The on-chip clearing process of a tumor spheroid on the microfluidic device.

Movie S2. Dynamic motility of lysosomes in the deeper layer of the spheroids.